Phytomedicine 60 (2019) 153010

Contents lists available at ScienceDirect

Phytomedicine

journal homepage: www.elsevier.com/locate/phymed

Original Article

Isolation, synthesis, and drug interaction potential of secondary metabolites derived from the leaves of miracle tree (*Moringa oleifera)* against CYP3A4 and CYP2D6 isozymes

Omer I. Fantoukh[a,b,c], Mohamed A. Albadry[a,b], Abidah Parveen[a,b,d], Mohammed F. Hawwal[a,b,c], Taghreed Majrashi[a,b], Zulfiqar Ali[a], Shabana I. Khan[a,b], Amar G. Chittiboyina[a], Ikhlas A. Khan[a,b,*]

[a] National Center for Natural Products Research, School of Pharmacy, The University of Mississippi, University, MS 38677, USA
[b] Division of Pharmacognosy, Department of BioMolecular Sciences, School of Pharmacy, The University of Mississippi, University, MS 38677, USA
[c] Department of Pharmacognosy, College of Pharmacy, King Saud University, Riyadh 4545, Saudi Arabia
[d] Department of Pharmaceutical Sciences, Abbottabad University of Science & Technology, Havelian, KPK, Pakistan

ARTICLE INFO

Keywords:
Moringa oleifera
Moringaceae
Rhamnopyranoside synthesis
Niazirin
Cytotoxicity
CYP inhibition

Abbreviations:
CC, column chromatography
CYP450, cytochrome P450
HDI, herb-drug interaction
M. oleifera, Moringa oleifera
MeOH, methanol

ABSTRACT

Background: *Moringa oleifera* Lam. is known as a drumstick tree that is widely cultivated in various subtropical and tropical provinces. Previous studies indicated that both aqueous and methanolic extracts of *M. oleifera* leaves have potent inhibitory effects on two major drug metabolizing Cytochrome P450 enzymes, namely, CYP3A4 and CYP2D6.

Purpose: The current study was aimed to isolate the secondary metabolites from *M. oleifera* and investigate their cytotoxicity and inhibitory effects on CYP3A4 and CYP2D6 to assess their herb-drug interaction (HDI) potential.

Methods: Chemical structure elucidation was achieved by interpreting the spectroscopic data (UV, IR, 1D, and 2D NMR experiments), confirming by HR-ESI-MS, and comparing with the previously reported data in the literature. All the isolates were evaluated for their cytotoxicity against a panel of cell lines (SK-MEL, KB, BT-549, SK-OV-3, VERO, LLC-PK1, and HepG2) and inhibition of two principal CYP isozymes (CYP3A4 and CYP2D6).

Results: Phytochemical investigation of *M. oleifera* leaves resulted in the isolation and characterization of one new compound, namely omoringone (**1**), along with twelve known secondary metabolites (**2–13**) belonging to several chemical classes including flavonoids, terpenoids, lignans, and phenylalkanoids. A plausible biosynthetic pathway for compound **1** was provided. Because of the low isolation yield and limited supply, omoringone (**1**) and niazirin (**12**) were successively synthesized. No cytotoxicity was observed on any of the tested cell lines up to 50 μM. The extract exhibited an inhibitory effect on CYP3A4 isoform (IC_{50} = 52.5 ± 2.5 μg/ml). Among the isolates, **1–4** and **7–9** inhibited CYP3A4 with the IC_{50} values ranging from 41.5 to 100 μM with no remarkable effect on CYP2D6 isozyme.

Conclusion: This work aided in ascertaining components of *M. oleifera* contributing to CYP3A4 inhibition exhibited by the extract using an *in vitro* assay. Nonetheless, further studies are warranted to determine the bioavailability of the phytochemicals and extrapolate these findings in more physiologically relevant conditions to further establish the clinical relevance of *in vitro* observations.

Introduction

Moringa oleifera Lam. is widely cultivated in various subtropical and tropical areas, and it is known as a drumstick or miracle tree that belongs to the monogeneric genus *Moringa* in Moringaceae family. *M. oleifera* is a widespread species among 13 others in the genus (Saini et al., 2016). Since 2001, the number of international congresses and scientific studies increased disseminating information about the incredible properties of this species. Ayurvedic traditional medicine claims that *M. oleifera* can prevent 300 diseases, and it has been called the miracle vegetable because all parts of *Moringa* such as pods, leaves, roots, and seeds have been exploited to treat a variety of ailments. Various biological activities such as antioxidant, antihypertensive, antimicrobial, antidiabetic, anticancer, anti-inflammatory along with immunomodulatory, cardioprotective, and hepatoprotective effects have been associated with *M. oleifera* (Leone et al., 2015; Stohs and

* Corresponding author.
E-mail addresses: oifantou@go.olemiss.edu (O.I. Fantoukh), ikhan@olemiss.edu (I.A. Khan).

https://doi.org/10.1016/j.phymed.2019.153010
Received 24 April 2019; Received in revised form 21 June 2019; Accepted 1 July 2019

Hartman, 2015).

Several substrates and xenobiotics are metabolized principally by a superfamily of enzymes called cytochrome P450 (CYP450). They are heme-containing monooxygenase enzymes responsible for the metabolism of clinical drugs and the conversion of the prodrug to the biologically active metabolites in the human body. The catalytic activity of CYP isozymes can be altered by other medicines or herbs which behave as either CYP inhibitors or inducers (Denisov et al., 2005). While the former can cause an accumulation of concomitant medicines leading to acute toxicity profiles, the latter reduce the effectiveness of the concurrent drugs by affecting their pharmacokinetic properties and eliminating them rapidly from the biological system. Despite the significance of other CYP isoforms, CYP3A4 and CYP2D6 are accountable in the metabolism of 50% of clinical drugs (Butterweck et al., 2004). Consequently, the safety and efficacy studies in terms of drug interaction potential and cytotoxicity of the phytochemicals derived from *M. oleifera* need to be performed bearing in mind the popularity and tremendous economic impact of this edible plant species.

Limited preceding studies displayed significant cytotoxicity properties for the extracts of leaves and barks against breast and colorectal cancer cell lines (Al-Asmari et al., 2015; Jung, 2014; Stohs and Hartman, 2015), and cytotoxicity against HepG2 cells was demonstrated only with the aqueous extract of *M. oleifera* leaves (IC_{50} = 6 mg/ml) (Monera et al., 2008). On the other hand, significant CYP3A4 inhibitory effects were observed, with IC_{50} values of 0.5 and 2.5 mg/ml for methanolic and aqueous extracts of the *M. oleifera* leaves, respectively with less inhibitory activities reported for the root extracts (IC_{50} > 10 mg/ml) (Monera et al., 2008). Another study confirmed that the aqueous extract of *M. oleifera* leaves has a potent inhibition on CYP3A4, concurring with the previous finding (Awortwe et al., 2014). Both ethanol and aqueous leaves extracts were found to inhibit human CYP1A2, CYP2D6, CYP2E1, and CYP3A4 activities *in vitro* in a dose-dependent manner with the potent inhibition exhibited against CYP1A2 isozyme (IC_{50} = 13.8 ± 9.8 μg/ml) (Taesotikul et al., 2010). A fluorescence study revealed that both the extract and chlorogenic acid had some inhibition of both isozymes CYP3A4 (IC_{50} = 127.36 ± 2.98 μg/ml and 133.73 ± 1.79 μg/ml) and CYP2D6 (146.50 ± 3.46 μg/ml and 159.22 ± 3.53 μg/ml), respectively, but less than their respective positive controls ketoconazole and quinidine (Ahmmed et al., 2015). The potential of nine selected widely used tropical medicinal herbs including *M. oleifera* in inhibiting human cytochrome P450 (CYP) isozymes was investigated in human liver microsomes. In this study, a twelve probe metabolites of nine probe substrates were monitored with UPLC/MS-MS, and *M. oleifera* leaves aqueous extract showed a weak inhibitory effect on CYP1A2 and CYP2C9 with IC_{50} > 100 μg/ml (Showande et al., 2018). Owing to its immune booster effect, nutraceuticals claimed to contain *M. oleifera* are administered concomitantly with anti-HIV medicines, and co-administration of *M. oleifera* at the traditional dose did not alter the steady-state pharmacokinetic of nevirapine (Monera-Penduka et al., 2017). However, *M. oleifera* altered the pharmacokinetics of antimalarial treatment, amodiaquine, in healthy human volunteers showing a significant decrease in the C_{max} after concurrent administration (Olawoye et al., 2018). Similarly, pharmacokinetic studies conducted in Swiss albino mice indicated that *M. oleifera* increased the plasma concentration of rifampicin when administered concurrently (Pal et al., 2011).

However, most of these studies were limited to the solvent extracts level but not conducted on the chemical constituents. Notably, further studies are vital to determine the phytochemical components of *M. oleifera* responsible for the interactions with the metabolism of clinical drugs if consumed simultaneously. Therefore, the current study aims mainly to isolate the secondary metabolites from *M. oleifera* and investigate the inhibitory effects of the extract and the isolates on two principal drug metabolizing enzymes (CYP3A4 and CYP2D6) through an *in vitro* inhibition assay using recombinant CYPs along with the potential of cytotoxicity effects on tumor and normal cell lines.

Materials and methods

General experimental procedures

The NMR spectra were obtained on Bruker Avance DRX spectrometer at 400 MHz for ^{1}H and 100 MHz for ^{13}C experiments. Other 2D experiments (DEPTQ135, COSY, HSQC, HMBC, and NOESY) were recorded using standard pulse instrument software. Dimethyl sulfoxide-d_6 or methanol-d_4 were used as the internal standards and residual solvents to obtain and calibrate the spectrum, respectively. High-resolution electrospray ionization mass spectra (HR-ESI-MS) were acquired by injection the samples directly to an Agilent Technologies 6200 series mass spectrometer in the positive and negative ion modes. The specific rotation was measured on the AUTOPOL IV Automatic Polarimeter (Rudolph, Hackettstown, NJ, USA). Agilent Technologies Cary 630 FTIR IR was used to record the IR spectra. The isolation and fractionation procedures were performed using column chromatography on silica gel (32–63 μ, Dynamic adsorbents Inc.), Sephadex LH20 (Sigma-Aldrich), or reversed-phase C-18 (Polar bond, J. T. Baker). The TLC was carried out on silica gel F254 aluminum sheet (20 × 20 cm, Fluka) or silica 60 RP-18 F254S aluminum sheet (20 × 20 cm, Merck). Savant Speed Vac Plus SC210A Concentrator was employed to concentrate and dry the samples. Visualization of the spots on TLC was done under UV light at 254 or 365 nm followed by spraying with vanillin-sulphuric acid reagent (1% vanillin dissolved in 10% H_2SO_4/ethanol) and then heating via heat gun. The solvents used in the isolation, fractionation, synthesis, and purification steps were purchased from Fisher Scientific (Fair Lawn, NJ).

Plant material

The dried leaves of *M. oleifera* were obtained from Dr. Bello M. Oluwasesan, Nigeria in August 2016. A specimen sample (NCNPR # 18332) was prepared and deposited by Dr. Vijayasankar Raman in the herbarium of NCNPR, School of Pharmacy, the University of Mississippi after authentication. The morphological and chemical properties were compared with the reference sample (NCNPR #11695) for the authentication process at the NCNPR.

Extraction and isolation of compounds

The dried leaves of *M. oleifera* species (671 g) were ground to a fine powder and extracted successively using continuous extraction method by percolation process with hexanes (4 *l* × 5 × 12 h), acetone (4 *l* × 5 × 12 h), and methanol (4 *l* × 5 × 12 h), respectively at room temperature. The methanol solution was then evaporated under reduced pressure at 40 °C to yield a dried methanolic crude extract (73.1 g). The crude extract of the methanol soluble portion was fractionated by vacuum liquid chromatography (VLC) over reversed phase C-18 column (25 cm × 10 cm) using water/methanol gradients to provide eleven fractions (Fr. 1–11). Fr. 4 (3.4 g) was further fractionated over sephadex LH-20 (78 cm × 5.5 cm) with methanol and subsequently subjected on repeated column chromatography (CC) [silica gel (93 cm × 3 cm), ethyl acetate/chloroform/methanol/water (15:8:4:1 and 6:4:4:1); silica gel (94 cm × 2.5 cm), ethyl acetate/chloroform/methanol/water (15:8:4:1 and 6:4:4:1); and silica gel (99 cm × 2.5 cm), ethyl acetate/chloroform/methanol/water (10:6:4:1)] followed by preparative TLC to yield astragalin (**4**, 5.1 mg), isolariciresinol-3a-*O*-*β*-D-glucopyranoside (**9**, 5.0 mg), (*E*)/(*Z*)-2-hexenyl-*β*-D-glucopyranoside (**10**, 40.1 mg), niazirin (**12**, 5.6 mg), benzyl-*β*-primeveroside (**11**, 41.8 mg), and methyl-4-(*α*-L-rhamnopyranosyloxy) benzylcarbamate (**13**, 4.7 mg). Fr. 5 (4.1 g) was subjected to CC on Sephadex LH-20 (78 cm × 5.5 cm) using methanol as an eluent followed by repeated CC [silica gel (89.5 cm × 4 cm), chloroform/methanol (9:1, 17:3, and 4:1); silica gel (90 cm × 2.7 cm), chloroform/methanol (9:1 and 4:1); and silica gel (75 cm × 2 cm), ethyl acetate/

Table 1
^{1}H (400 MHz) and ^{13}C (100 MHz) NMR spectroscopic data of compound **1** (in MeOD, δ in ppm, *J* in Hz).

Position	Multiplicity	^{1}H (δ)	^{13}C (δ)
1	CH_3	2.38 (3H, s)	27.2
2	CO		201.3
3	CH	6.71 (1H, d, *J* = 16.3 Hz)	126.3
4	CH	7.64 (1H, d, *J* = 16.3 Hz)	145.4
1′	C		129.8
2′, 6′	CH	7.61 (2H, d, *J* = 8.7 Hz)	131.2
3′, 5′	CH	7.14 (2H, d, *J* = 8.7 Hz)	117.8
4′	C		159.8
1″	CH	5.52 (1H, d, *J* = 1.7 Hz)	99.6
2″	CH	4.03 (1H, dd, *J* = 3.4, 1.8 Hz)	71.9
3″	CH	3.86 (1H, dd, *J* = 9.4, 3.5 Hz)	72.2
4″	CH	3.49 (1H, t, *J* = 9.4 Hz)	73.7
5″	CH	3.65 – 3.57 (1H, m)	70.9
6″	CH_3	1.24 (3H, d, *J* = 6.1 Hz)	18.0

Table 2
^{1}H (400 MHz) and ^{13}C (100 MHz) NMR spectroscopic data of compound **12** (in MeOD, δ in ppm, *J* in Hz).

Position	Multiplicity	^{1}H (δ)	^{13}C (δ)
1	CN		120.0
2	CH_2	3.81 (2H, s)	22.8
1′	C		125.6
2′, 6′	CH	7.27 (2H, d, *J* = 8.6 Hz)	130.3
3′, 5′	CH	7.07 (2H, d, *J* = 9.6 Hz)	118.0
4′	C		157.2
1″	CH	5.47 (1H, d, *J* = 1.9 Hz)	99.6
2″	CH	4.07 (1H, dd, *J* = 3.4, 1.9 Hz)	71.8
3′	CH	3.91 (1H, dd, *J* = 9.5, 3.6 Hz)	72.1
4″	CH	3.51 (1H, t, *J* = 9.5 Hz)	73.7
5″	CH	3.69 – 3.61 (1H, m)	70.6
6″	CH_3	1.24 (2H, d, *J* = 6.3 Hz)	18.1

chloroform/methanol/water (15:8:4:1)] to afford omoringone (**1**, 1.5 mg), rutin (**2**, 117.2 mg), isoquercitrin (**3**, 792.1 mg), lariciresinol-9-*O*-*β*-D-glucopyranoside (**7**, 28.9 mg), and (+)-pinoresinol-4-*O*-*β*-D-glucopyranoside (**8**, 10.3 mg). Fr. 7 (1.5 g) was applied to CC over Sephadex LH-20 (78 cm × 5.5 cm) eluted with methanol and subsequently applied on normal phase silica gel (92 cm × 3.25 cm) using ethyl acetate/chloroform/methanol/water gradient (15:8:4:1) to purify (*S*) linalyl-*β*-D-glucopyranoside (**5**, 5.3 mg) and (*S*) linalyl-*β*-primeveroside (**6**, 24.2 mg). Chemical Structure elucidation of the isolated compounds was performed by analysis of their spectroscopic data including 1D and 2D NMR and confirmed by HR-ESI-MS spectrometric analysis.

Omoringone (**1**): semisolid; UV (CH_3OH) λ_{max} nm 313.2, 229.6 nm; ^{1}H and ^{13}C NMR (CD_3OD), see Table 1; positive HR-ESI-MS *m/z* 309.1328 (calcd. for $[C_{16}H_{20}O_6 + H]^+$, 309.1338).

Chemical synthesis of intermediates and compounds

1, 2, 3, 4-tetra-O-acetate-L-rhamnopyranoside (15)

L-rhamnose monohydrate (**14**) (2.5 g, 15.23 mmol, 1 equiv.) and a catalytic amount of DMAP (4-dimethyl aminopyridine) (186 mg, 1.52 mmol, 0.1 equiv.) were dissolved in anhydrous pyridine (8.9 ml). Then, acetic anhydride (10.4 ml) was added to the solution and stirred for 16 h at room temperature under N_2 atmosphere. After completion of the reaction, the crude mixture was concentrated, and the excess pyridine was co-evaporated with toluene. The mixture was dissolved in EtOAc, and washed with 1.0 N HCl, $NaHCO_3$, and brine (aqueous 5% NaCl), respectively. The organic layer was dried over anhydrous Mg_2SO_4 and co-evaporated with toluene (2 times).

2, 3, 4-tri-O-acetate-L-rhamnopyranose hemiacetal (16)

Hydrazine acetate (0.27 g, 3.01 mmol, 1.1 equiv.) was added to a solution of 1, 2, 3, 4-tetra-*O*-acetate-L-rhamnopyranoside (**15**) (1 g, 3.01 mmol, 1 equiv.) in DMF (13 ml) at 50 °C and stirred the reaction for 2 h under N_2. Upon disappearance of starting material (TLC), the mixture was diluted with EtOAc and washed with brine. The organic layer was dried over anhydrous Mg_2SO_4 and concentrated to give a yellow oily product.

2, 3, 4-tri-O-acetate-α-L-rhamnosyl trichloro acetimidate (17)

To a solution of 2, 3, 4-tri-*O*-acetate-L-rhamnopyranose hemiacetal (**16**) (0.87 g, 3 mmol, 1 equiv.) in anhydrous DCM (10 ml) trichloroacetonitrile (2.71 ml, 27 mmol, 9 equiv.) and DBU (0.16 g, 1.05 mmol, 0.35 equiv.) were added successively. The resulting mixture was stirred for 2h at RT, concentrated using rotary evaporator and the resulting crude product was utilized without further purification.

Synthesis of omoringone (1)

2, 3, 4-tri-*O*-acetate-α-L-rhamnosyl trichloro acetimidate (**17**) (0.325 g, 0.75 mmol, 1 equiv.) and 4-hydroxy benzylidene acetone (**18**) (0.14 g, 0.90 mmol, 1.2 equiv.) with molecular sieves (3 Å) were taken in freshly distilled dichloromethane (DCM) (10 ml) at 0 °C and stirred for 30 min under N_2 atmosphere. Trimethylsilyl trifluoromethanesulfonate (TMSOTf) (135.11 µl, 0.75 mmol, 1 equiv.) was added dropwise to the reaction mixture at 0 °C and slowly allowed the reaction mixture to RT and stirred for overnight. After completion of all the starting materials based on TLC, the reaction mixture was filtered and dissolved in $CHCl_3$ (30 ml). The organic layer was washed with aq. $NaHCO_3$ solution, dried over anhydrous Mg_2SO_4 and concentrated under reduced pressure to provide 4-[(2,3,4-tri-*O*-acetyl-*α*-L-rhamnopyranosyl)oxy]-benzylidene acetone (**19**). The resulting crude product was dissolved in anhydrous methanol that contained a catalytic amount of sodium methoxide (350 µl). The reaction mixture was allowed to stir at ambient temperature for 30 min under N_2. After total consumption of starting material, the reaction mixture was neutralized by the addition of Amberlite IR-120 (H^+) resin. Then, the reaction mixture was filtered and concentrated under reduced pressure to obtain a crude product containing omoringone (**1**). The crude product was purified by silica gel chromatography using a gradient of chloroform: methanol (9: 1, v/v) to obtain omoringone (**1**) as a semisolid (12 mg, 62%).

Synthesis of niazirin (12)

2, 3, 4-tri-*O*-acetate-α-L-rhamnosyl trichloro acetimidate (**17**) (0.325 g, 0.75 mmol, 1 equiv.) and 4-hydroxy benzene acetonitrile (**20**) (0.12 g, 0.90 mmol, 1.2 equiv.) with molecular sieves (3 Å) were taken in freshly distilled DCM (10 ml) at 0 °C and stirred for 30 min under N_2 atmosphere. To this reaction mixture, TMSOTf (135.11 µl, 0.75 mmol, 1 equiv.) was added dropwise at 0 °C and slowly allowed the reaction mixture to RT and stirred for overnight. After completion of all the starting materials based on TLC, the reaction mixture was filtered and dissolved in $CHCl_3$ (30 ml). The organic layer was washed with aq. $NaHCO_3$ solution, dried over anhydrous Mg_2SO_4 and concentrated under reduced pressure to provide 4-[(2,3,4-tri-*O*-acetyl-*α*-L-rhamnopyranosyl)oxy]-benzeneacetonitrile (**21**). This mixture containing compound **21** was dissolved in anhydrous methanol containing a catalytic amount of sodium methoxide (200 µl). The reaction mixture was allowed to stir at ambient temperature for 30 min under N_2. After total consumption of starting material, the reaction mixture was neutralized by the addition of Amberlite IR-120 (H^+) resin to neutralize the mixture. Then, the reaction mixture was filtered and concentrated under reduced pressure to obtain a crude product containing niazirin (**12**). The crude product was purified by silica gel chromatography using a gradient of chloroform: methanol (9: 1, v/v) to obtain niazirin (**12**) as a semisolid (62 mg, 62%).

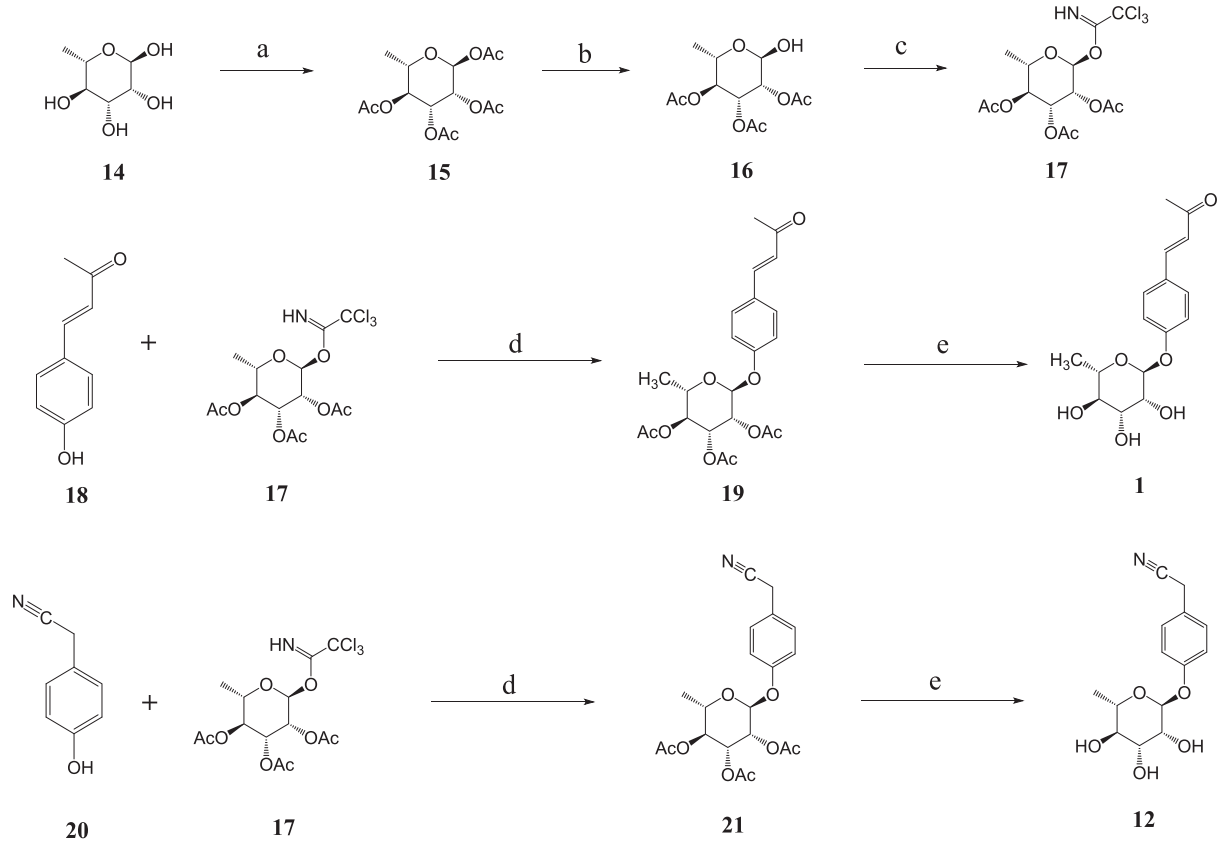

Scheme 1. Synthesis of compounds **1** and **12**.
Reagents and conditions: (a) Ac_2O, Pyridine, DMAP, 25 °C, 16 h (91%); (b) hydrazine acetate, DMF, 55 °C, 4 h, (84%); (c) CCl_3CN, DBU, DCM, 0–25 °C, 2 h, (63%); (d) (1) CH_2Cl_2, 10 min, 0 °C; (2) $Me_3SiSO_3CF_3$, 3 h, 0 °C, (40%); (e) Anhydrous MeOH, CH_3ONa, 10 min, 25 °C (30–35%).

Table 3
Inhibition of CYP3A4 and CYP2D6 isozymes by *M. oleifera* extract and isolated compounds. Values are IC_{50} in μg/ml for extract and μM for compounds.

	Test sample	CYP3A4	CYP2D6
	M. oleifera MeOH extract	52.5 ± 2.5	–
1	(*E*) − 4-[4-[(*β*-D-glucopyranosyl)oxy]phenyl]but-3-en-2-one	41.5 ± 3.5	>100
2	Rutin	60 ± 5	–
3	Isoquercitrin	65.5 ± 4.5	>100
4	Astragalin	69.5 ± 1.5	90 ± 5
5	(*S*) Linalyl-*β*-D-glucoside	–	–
6	(*S*) Linalyl-*β*-primeveroside	–	>100
7	Lariciresinol-9-*O*-*β*-D-glucopyranoside	72.5 ± 7.5	–
8	(+)-Pinoresinol-4-*O*-*β*-D-glucopyranoside	41.5 ± 3.2	–
9	Isolariciresinol-3a-*O*-*β*-D-glucopyranoside	100 ± 0	–
10	(*E*)/(*Z*) − 2-Hexenyl-*β*-D-glucopyranoside	–	–
11	Benzyl-*β*-primeveroside	> 100	> 100
12	Niazirin	–	–
13	Methyl-4-(*α*-L-rhamnopyranosyloxy)benzylcarbamate	>100	>100
	Ketoconazole$^{\Omega}$	0.040 ± 0.006	
	Quinidine$^{\Omega}$		0.050 ± 0.004

(-) indicates the lack of inhibition, ($^{\Omega}$) indicates the positive control for respective CYP450 isozyme. The data are represented as mean ± SEM of three independent experiments.

Cytotoxicity assay

The isolated phytochemicals were evaluated for their cytotoxicity towards four human solid tumor cell lines (melanoma: SK-MEL, epidermal carcinoma: KB, breast ductal carcinoma: BT-549, and ovarian carcinoma: SK-OV-3), and three kidney and liver cell lines (African green monkey kidney fibroblast: VERO, pig kidney epithelial: LLC-PK1 and human hepatoma cells: HepG2). DMSO and doxorubicin were included as negative and positive controls, respectively. The assay was performed in 96-well tissue culture-treated microplates as described earlier (Zulfiqar et al., 2017). In brief, cells were seeded to the wells of the plate at a density of 10,000 cells/well and incubated for 24 h before treating with various concentrations of the test samples and incubating for 48 h. Cell viability was determined using the tetrazolium dye (WST-8). IC_{50} values were calculated from concentration-response curves of % decrease in cell viability *vs.* test concentrations.

Inhibition of the catalytic activity of CYP3A4 and CYP2D6

The assay to determine the inhibition of the catalytic activity of

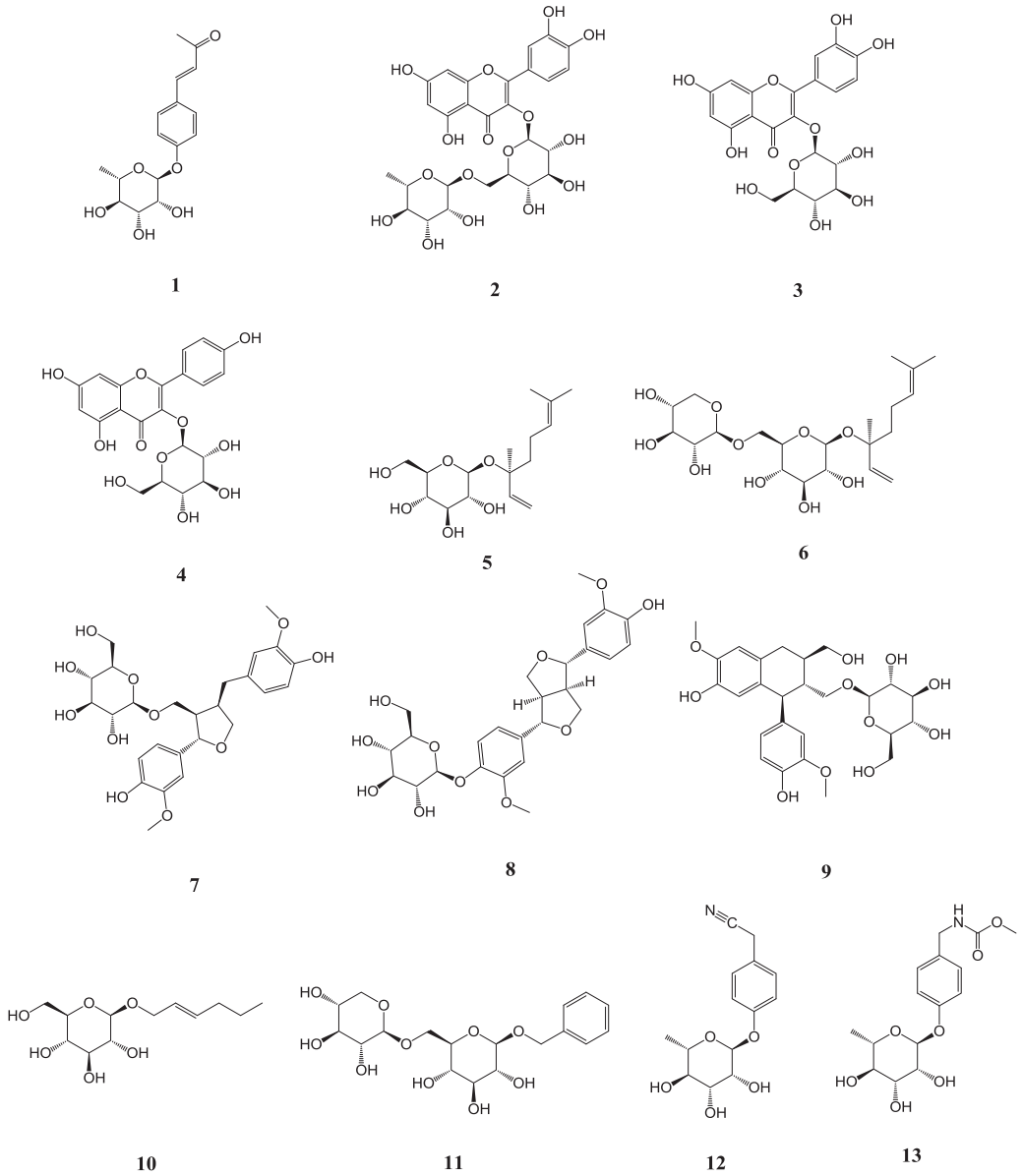

Fig. 1. Chemical structures of isolated phytoconstituents **1–13** from *M. oleifera*.

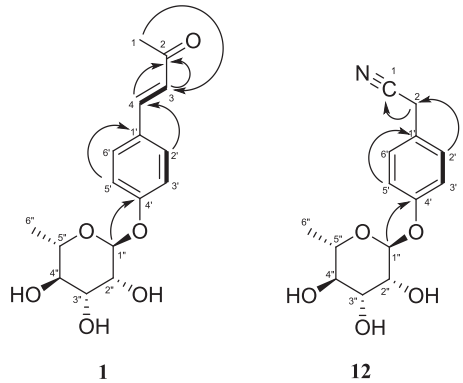

Fig. 2. The key HMBC (arrows) and $^{1}H–^{1}H$ COSY (bold lines) correlations of compounds **1** and **12**.

CYPs was performed using CYP3A4/BFC and CYP2D6/AMMC inhibitor screening kits (Corning Life Sciences) as reported earlier with some modifications (Fantoukh et al., 2019). The fluorescent substrates were 7-benzyloxy-trifluoromethyl coumarin (BFC) and 3-[2-(N,N-diethyl-N-methylamino)ethyl] – 7-methoxy-4-methylcoumarin (AMMC) for CYP3A4 and CYP2D6, respectively. The extract of *M. oleifera* and its constituents were dissolved in methanol and serially diluted in a solution (100 µl) of cofactors mix, CYP proteins (0.05 mg of protein/ml), and G-6-PDH to achieve six concentrations ranging from 0.1 to 100 µg/ml for the extract and 0.1 to 100 µM for the pure compounds. The highest concentration of methanol was 1% (vehicle control). Initial readings were recorded to report the inherent fluorescence before incubating the plates at 37 °C for 10 min. Initiation of the enzymatic reaction was achieved by the addition of the enzyme substrate mixture (100 µl) followed by incubation for 30 min at 37 °C. The enzymatic reaction was terminated by the addition of 75 µl of ice cold acetonitrile/0.5 M Tris base (80:20). Fluorescence was measured on a Spectramax M5 plate reader (Molecular Devices, Sunnyvale, CA, USA) at excitation/emission wavelengths of 409 / 530 nm to detect 7-hydroxytrifluoromethyl coumarin (HFC) and 390 / 460 nm to detect 3-[2-(N,N-diethylamino)ethyl] – 7-hydroxy-4-methyl coumarin hydrochloride (AHMC) as metabolites of BFC and AMMC, respectively. The inhibitory potential was reported in terms of IC_{50} values, obtained from

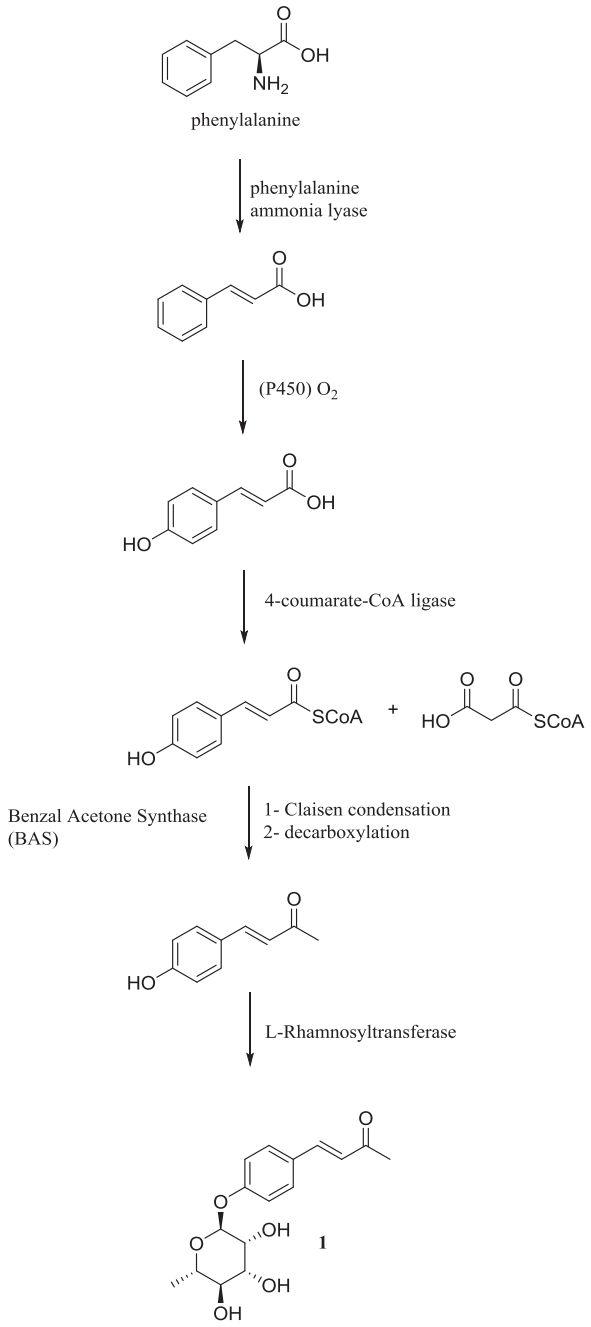

Scheme 2. Plausible biosynthetic pathway for compound **1**.

concentration-response curves generated by plotting the tested concentrations against enzyme inhibition (%) using Microsoft Excel.

Results

Isolation and structure elucidation

All isolated secondary metabolites were obtained from the methanol soluble portion of *M. oleifera* leaves by repeated column chromatographic techniques (silica gel, RP-18 silica gel, and Sephadex LH-20) as well as preparative TLC over silica gel. Phytochemical investigation of MeOH extract for *M. oleifera* leaves resulted in the isolation and characterization of one new benzyl acetone rhamnoside, namely omoringone (**1**), together with 12 known secondary metabolites (**2–13**). Based on the extensive spectroscopic (1D and 2D NMR) and spectrometric (HR-ESI-MS) analysis, known compounds were identified as rutin (**2**), isoquercitrin (**3**), astragalin (**4**), (*S*) linalyl-*β*-D-glucoside (**5**), (*S*) linalyl-*β*-primeveroside (**6**), lariciresinol-9-*O*-*β*-D-glucopyranoside (**7**), (+)-pinoresinol-4-*O*-*β*-D-glucopyranoside (**8**), isolariciresinol-3a-*O*-*β*-D-glucopyranoside (**9**), (*E*)/(*Z*)-2-hexenyl-1-*O*-*β*-D-glucopyranoside (**10**), benzyl-*β*-primeveroside (**11**), niazirin (**12**), and methyl-4-(*α*-L-rhamnopyranosyloxy)benzylcarbamate (**13**) (Fig. 1). The NMR data (^{1}H, ^{13}C, DEPT135) for compounds **1** and **12** are shown in Tables 1 and 2, respectively.

*Synthesis of compounds **1** and **12***

Compounds **1** and **12** were synthesized to obtain sufficient material for performing biological tests. Our chemical synthesis scheme for compounds **1** and **12** starts with L-rhamnose monohydrate with acetylation step followed by regioselective deprotection of the anomeric position and subsequently lead to the trichloroacetimidate derivative as rhamnosyl donor. The latter reacts with either 4-hydroxy benzylidene acetone or 4-hydroxy benzene acetonitrile to produce omoringone (**1**) or niazirin (**12**), respectively, as described in Scheme 1.

Cytotoxicity screening

All the isolates were evaluated for their cytotoxicity against a panel of cancer and noncancer cell lines (SK-MEL, KB, BT-549, SK-OV-3, Vero, LLC-PK1, and HepG2). No cytotoxicity effects were observed on any of the tested cell lines up to a highest concentration of 50 μM (data not shown).

Inhibition of CYP isoforms by the MeOH extract of M. oleifera and its isolated compounds

The inhibitory effects of test samples on the catalytic activity of two major CYP isoforms (CYP3A4 and CYP2D6) were measured. A decrease in the formation of the respective probe metabolites was calculated, and the IC_{50} value (concentration responsible for a 50% decrease in activity) was determined from concentration-response curves. The crude methanolic extract of *M. oleifera* exhibited a remarkable inhibition (IC_{50} = 52.50 ± 2.5 μg/ml) of CYP3A4 with no effect on CYP2D6 at 100 μg/ml. It was interesting to note that the activity of CYP3A4 was inhibited by compounds **1–4** and **7–9** in varying degrees with IC_{50} values ranging from 41.5 to 100 μM with no remarkable effect observed on the activity of CYP2D6 isozyme making them the potential major contributors for the inhibitory activity of the extract against CYP3A4 as shown in Table 3.

Discussion

Owing to the ethnobotanical significance of this plant species, the prime research aims to assess the phytochemical profile, the cytotoxic effect, and drug interaction potential for the extract and isolated secondary metabolites from *M. oleifera*. All isolated compounds were obtained from the methanol soluble portion of *M. oleifera* leaves by column chromatography using various matrices (silica gel, RP-18 silica gel, and Sephadex LH-20) as well as preparative TLC over silica gel. The isolated compounds represent a variety of chemical classes such as flavonoid, terpenoid, lignan, and other phenolic components (Fig. 1). To the best of our knowledge, compound **1** was found to be a new metabolite. Also, this is the first isolation report for compounds **5–10** from this species. In addition, compounds **12** and **13** are unique components of *M. oleifera*, and they could be employed as analytical markers for the chemical fingerprinting profile and quality control for herbal supplements claiming to contain this plant species.

The molecular formula of compound **1** was determined as $C_{16}H_{20}O_6$ which was compatible with the protonated molecule at *m/z* 309.1328 (calcd. for $[C_{16}H_{20}O_6 + H]^+$, 309.1338) in the HRESIMS and displayed seven degrees of unsaturation. Investigation of HSQC, COSY, and HMBC

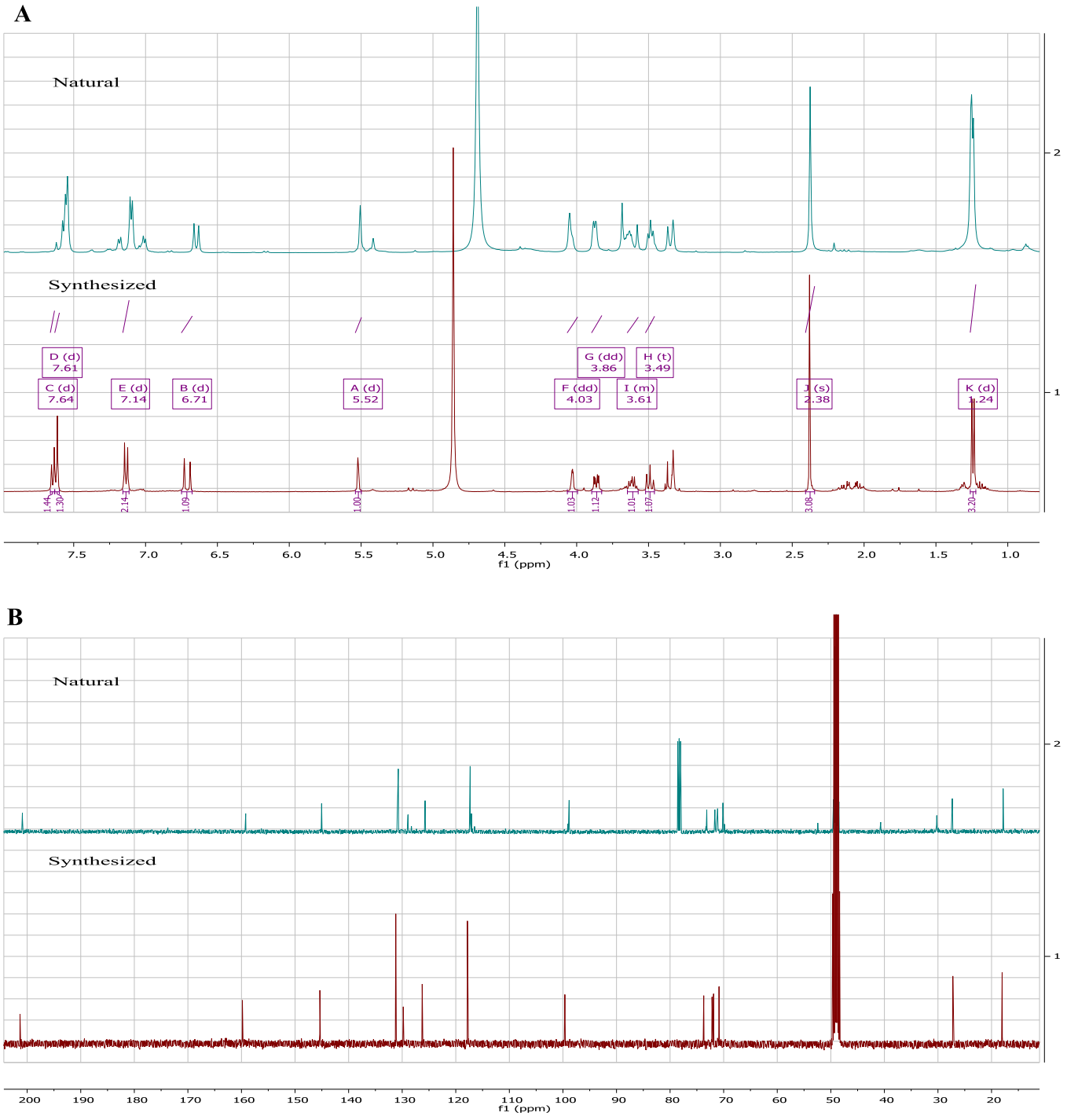

Fig. 3. (A) Comparisons of ^{1}H NMR spectra for natural and synthesized omoringone (**1**). (B) Comparisons of ^{13}C NMR spectra for natural and synthesized omoringone (**1**).

spectra allowed assigning the ^{1}H NMR and ^{13}C NMR spectroscopic data. Decoupled ^{13}C NMR spectrum exhibited sixteen resonances which were distinguished as two methyl, eleven methine, and three non-protonated carbons using DEPTQ135 experiment. Among them, the compound includes a carbonyl moiety (201.3 ppm) and one deoxyhexose sugar unit which was identified as *α*-L-rhamnopyranose based on coupling constants $^{3}J_{\text{H-1}'',\ \text{H-2}''} = 1.7$ Hz of anomeric proton alongside the other characteristic ^{13}C NMR chemical shift values. Besides, ^{1}H NMR displayed AB spin system characterized by roofing effect indicating aromatic ring with symmetry as 1, 4-disubstituted benzene. Two additional ethylenic carbons were observed (126.3 and 145.4 ppm) which revealed the existence of a double bond. Its geometry was assigned as *(E)* configuration based on the high *J*-value between the vicinal protons (16.3 Hz). A singlet (3H) at 2.38 ppm in the ^{1}H NMR spectrum was indicative of the presence of an acetyl group. The HMBC cross-peak correlations of the anomeric proton for (δ_H 5.52) with C-4′ (δ_C 159.8) indicated that glycone residue was located at C-4′ (Fig. 2). All this data was evident to elucidate the structure as (*E*) − 4-[4-[(*α*-L-rhamnopyranosyl)oxy]phenyl]but-3-en-2-one.

A putative proposed biosynthesis for compound **1** is illustrated in Scheme 2. It is biosynthesized from the shikimic acid pathway via conversion of the phenylalanine moiety to cinnamic acid by

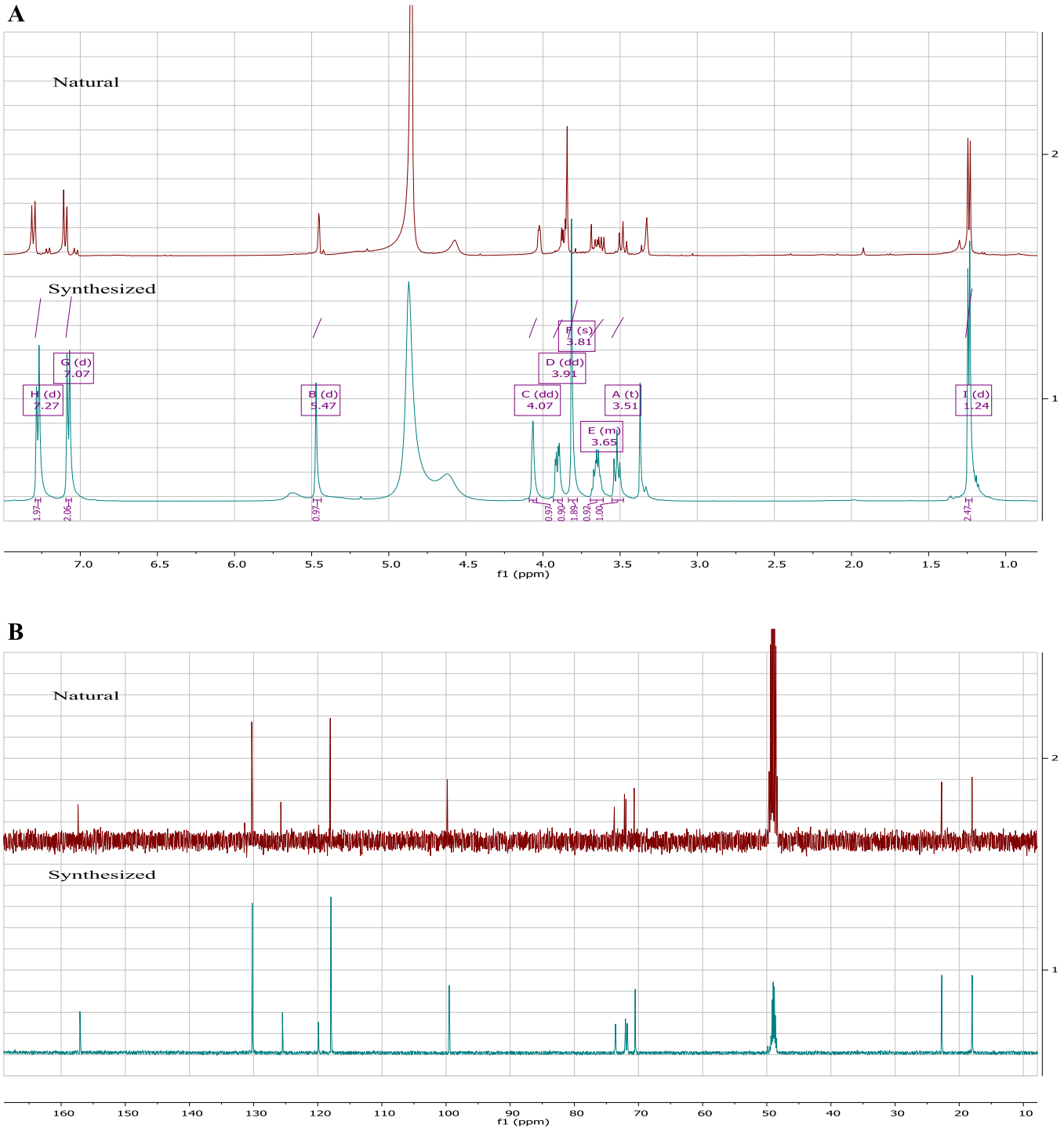

Fig. 4. (A) Comparisons of ^{1}H NMR spectra for natural and synthesized niazirin (**12**). (B) Comparisons of ^{13}C NMR spectra for natural and synthesized niazirin (**12**).

phenylalanine ammonia lyase followed by aromatic hydroxylation via CYP450 to provide *p*-coumaric acid. The latter was catalyzed by *P*-coumarate-CoA ligase to yield *p*-coumaroyl-CoA. Benzalacetone synthase forms the polyketide intermediate *p*-hydroxybenzalacetone through the decarboxylative (Claisen-type) condensation of *p*-coumaroyl-CoA with malonyl-CoA, followed by hydrolysis and decarboxylation (Koeduka et al., 2011). In the presence of rhamnosyl transferase as tailoring enzyme, the glycone moiety was incorporated into the benzalacetone basic skeleton to provide compound **1**.

Because of the low isolation yields, compounds **1** and **12** were successfully synthesized to obtain sufficient material for performing biological tests. This work constitutes the first synthesis for compounds **1** and **12**. Comparisons of ^{1}H NMR spectra for natural and synthesized omoringone (**1**) and niazirin (**12**) are illustrated in Figs. 3A, and 4A, respectively. Comparisons of ^{13}C NMR spectra of natural and synthesized omoringone (**1**) and niazirin (**12**) are shown in Figs. 3B, and 4B, respectively.

Multiple endogenous substrates and exogenous xenobiotics are predominantly metabolized and biosynthesized by cytochrome P450. These heme-containing mono-oxygenases are exclusively responsible for the conversion of the inactive prodrug to the pharmacologically active metabolites in the human body (Denisov et al., 2005). CYP

inhibitors and inducers interact with CYP isozymes in the binding site leading to interference with their substrates and drugs. Particularly, CYP inhibitors can intensify the toxicity profile while the CYP inducers can increase the clearance of the co-administered drugs affecting their therapeutic effectiveness. (Butterweck et al., 2004). Although *M. oleifera* extracts indicate a high degree of safety, and no adverse effects were reported in humans so far, some studies highlighted that the chronic administration of *M. oleifera* extracts might distort the histoarchitecture of both liver and kidneys which predispose to hepatic and kidney damage and ultimately lead to hepatotoxicity and nephrotoxicity (Ambi et al., 2011; Awodele et al., 2012; Oyagbemi et al., 2013; Paul CW, 2012). In the current study, we investigated the inhibitory activities of the extract and isolated secondary metabolites from *M. oleifera* against two principal CYP450 isozymes (CYP3A4 and CYP2D6) which are responsible for 50% of clinical drug metabolism. The new compound, namely omoringone (**1**), in addition to the flavonols **2–4**, and lignans **7–9** exhibited the strongest inhibition against CYP3A4 ranging from 41.5 to 100 μM. Except for astragalin (**4**) which exhibited a weak inhibitory activity on CYP2D6 (IC_{50} = 90 ± 5 μM), no remarkable inhibitory activity was shown against CYP2D6 by the tested samples. On the other hand, the monoterpenoids **5** and **6** in addition to compounds **10–13** displayed no effect on both isozymes. Even though the flavonoids such as rutin and isoquercitrin show different *in vitro* IC_{50} values, they are expected to exert similar inhibitory effects in the animal model. This effect could be a consequence for the conversion of the aforementioned flavonols to flavonol aglycone derivative, quercetin. The latter was extensively evaluated and found to inhibit several CYP isozymes including CYP3A4, CYP2D6, and CYP2C9 according to prior *in vivo* studies (Song et al., 2013; Valentova et al., 2014). Despite the fact that compounds **12** and **13** are unique and might be considered as analytical markers for *M. oleifera*, they exhibited no inhibitory effects on both CYP isozymes tested as mentioned earlier. Although *M. oleifera* extract and its isolated phytochemicals were tested against an array of the tumor and normal cell lines, they demonstrated no cytotoxicity effects for the extract and its constituents at 50 μg/ml and 50 μM, respectively. The results indicate that *M. oleifera* and its tested phytoconstituents are less potential to be developed as anticancer agents. In addition, the results suggest that *M. oleifera* and its tested ingredients are potentially safe against normal cells such as kidney and liver. This work aided in ascertaining components in *M. oleifera* with potential HDI using *in vitro* methods for CYP inhibition. Nonetheless, further studies should be conducted to determine the bioavailability of the phytochemicals and extrapolate the findings to *in vivo* animal model.

In conclusion, 13 secondary metabolites were isolated from *M. oleifera* leaves. Omoringone (**1**) was found to be a new metabolite. Omoringone (**1**) and niazirin (**12**) were successively synthesized to provide sufficient quantities for conducting the additional bioassays. This work also constitutes the first synthesis for the two aforementioned compounds. No cytotoxicity effects were observed on any tested cell lines at 50 μg/ml and 50 μM for the extract and phytochemicals, respectively. The extract inhibited CYP3A4 catalytic activity (IC_{50} = 52.5 ± 2.5 μg/ml) with inhibitory effects observed only with the compounds **1–4** and **7–9** on CYP3A4 with IC_{50} ranging from 41.5 to 100 μM while no remarkable effect was observed on CYP2D6 isozyme.

Conflict of interest

The authors declare that relationships leading to a potential conflict of interest such as commercial or financial were absent in this research.

Acknowledgments

This research was supported by Science-Based Authentication of Dietary Supplements funded by the Food and Drug Administration grant number [5U01FD004246-07]. Omer and Mohammed extend their appreciation to the Deanship of Scientific Research and the Research Center, College of Pharmacy, King Saud University for financial support.

References

Ahmmed, S.M., Mukherjee, P.K., Bahadur, S., Kar, A., Al-Dhabi, N.A., Duraipandiyan, V., 2015. Inhibition potential of *Moringa oleifera* Lam. on drug metabolizing enzymes. Indian J. Tradit. Knowl.

Al-Asmari, A.K., Albalawi, S.M., Athar, M.T., Khan, A.Q., Al-Shahrani, H., Islam, M., 2015. *Moringa oleifera* as an anti-cancer agent against breast and colorectal cancer cell lines. PLoS One 10 (8), e0135814. https://doi.org/10.1371/journal.pone.0135814.

Ambi, AA, A., E., Umar, A, Katsayal, UA, Sule, MI, Pateh, UU, et al., 2011. Toxicity evaluation of *Moringa oleifera* leaves. Int. J. Pharmaceut. Res. Innovat. 4, 22–24.

Awodele, O., Oreagba, I.A., Odoma, S., da Silva, J.A., Osunkalu, V.O., 2012. Toxicological evaluation of the aqueous leaf extract of *Moringa oleifera* Lam. (Moringaceae). J. Ethnopharmacol. 139 (2), 330–336. https://doi.org/10.1016/j.jep.2011.10.008.

Awortwe, C., Bouic, P.J., Masimirembwa, C.M., Rosenkranz, B., 2014. Inhibition of major drug metabolizing CYPs by common herbal medicines used by HIV/AIDS patients in Africa- implications for herb-drug interactions. Drug Metab. Lett. 7 (2), 83–95.

Butterweck, V., Derendorf, H., Gaus, W., Nahrstedt, A., Schulz, V., Unger, M., 2004. Pharmacokinetic herb-drug interactions: are preventive screenings necessary and appropriate? Planta Med. 70 (9), 784–791. https://doi.org/10.1055/s-2004-827223.

Denisov, I.G., Makris, T.M., Sligar, S.G., Schlichting, I., 2005. Structure and chemistry of cytochrome P450. Chem. Rev. 105 (6), 2253–2277. https://doi.org/10.1021/cr0307143.

Fantoukh, O.I., Dale, O.R., Parveen, A., Hawwal, M.F., Ali, Z., Manda, V.K., Khan, S.I., Chittiboyina, A.G., Viljoen, A., Khan, I.A., 2019. Safety assessment of phytochemicals derived from the globalized South African rooibos tea (*Aspalathus linearis*) through interaction with CYP, PXR, and P-gp. J. Agric. Food Chem. 67 (17), 4967–4975. https://doi.org/10.1021/acs.jafc.9b00846.

Jung, I.L., 2014. Soluble extract from *Moringa oleifera* leaves with a new anticancer activity. PLoS One 9 (4), e95492. https://doi.org/10.1371/journal.pone.0095492.

Koeduka, T., Watanabe, B., Suzuki, S., Hiratake, J., Mano, J., Yazaki, K., 2011. Characterization of raspberry ketone/zingerone synthase, catalyzing the α, β-hydrogenation of phenylbutenones in raspberry fruits. Biochem. Biophys. Res. Commun. 412 (1), 104–108. https://doi.org/10.1016/j.bbrc.2011.07.052.

Leone, A., Spada, A., Battezzati, A., Schiraldi, A., Aristil, J., Bertoli, S., 2015. Cultivation, genetic, ethnopharmacology, phytochemistry and pharmacology of *Moringa oleifera* leaves: an overview. Int. J. Mol. Sci. 16 (6), 12791–12835. https://doi.org/10.3390/ijms160612791.

Monera-Penduka, T.G., Maponga, C.C., Wolfe, A.R., Wiesner, L., Morse, G.D., Nhachi, C.F., 2017. Effect of *Moringa oleifera* Lam. leaf powder on the pharmacokinetics of nevirapine in HIV-infected adults: a one sequence cross-over study. AIDS Res. Ther. 14, 12. https://doi.org/10.1186/s12981-017-0140-4.

Monera, T.G., Wolfe, A.R., Maponga, C.C., Benet, L.Z., Guglielmo, J., 2008. *Moringa oleifera* leaf extracts inhibit 6β-hydroxylation of testosterone by CYP3A4. J. Infect. Dev. Ctries. 2 (5), 379–383.

Olawoye, O.S., Adeagbo, B.A., Bolaji, O.O., 2018. *Moringa oleifera* leaf powder alters the pharmacokinetics of amodiaquine in healthy human volunteers. J. Clin. Pharm. Ther. 43 (5), 626–632. https://doi.org/10.1111/jcpt.12725.

Oyagbemi, A.A., Omobowale, T.O., Azeez, I.O., Abiola, J.O., Adedokun, R.A., Nottidge, H.O., 2013. Toxicological evaluations of methanolic extract of *Moringa oleifera* leaves in liver and kidney of male Wistar rats. J. Basic Clin. Physiol. Pharmacol. 24 (4), 307–312. https://doi.org/10.1515/jbcpp-2012-0061.

Pal, A., Bawankule, D.U., Darokar, M.P., Gupta, S.C., Arya, J.S., Shanker, K., Gupta, M.M., Yadav, N.P., Singh Khanuja, S.P., 2011. Influence of *Moringa oleifera* on pharmacokinetic disposition of rifampicin using HPLC-PDA method: a pre-clinical study. Biomed. Chromatogr. 25 (6), 641–645. https://doi.org/10.1002/bmc.1494.

Paul, CW, D., B., 2012. The effect of methanolic extract of *Moringa oleifera* lam roots on the histology of kidney and liver of guinea pigs. Asian J. Med. Sci. 4, 55–60.

Saini, R.K., Sivanesan, I., Keum, Y.S., 2016. Phytochemicals of*Moringa oleifera*: a review of their nutritional, therapeutic and industrial significance. 3 Biotech 6 (2), 203. https://doi.org/10.1007/s13205-016-0526-3.

Showande, S.J., Fakeye, T.O., Kajula, M., Hokkanen, J., Tolonen, A., 2018. Potential inhibition of major human cytochrome P450 isoenzymes by selected tropical medicinal herbs—implication for herb–drug interactions. Food Sci. Nutr. 0 (0). https://doi.org/10.1002/fsn3.789.

Song, M., Hong, M., Lee, M.Y., Jee, J.G., Lee, Y.M., Bae, J.S., Jeong, T.C., Lee, S., 2013. Selective inhibition of the cytochrome P450 isoform by hyperoside and its potent inhibition of CYP2D6. Food Chem. Toxicol. 59, 549–553. https://doi.org/10.1016/j.fct.2013.06.055.

Stohs, S.J., Hartman, M.J., 2015. Review of the safety and efficacy of *Moringa oleifera*. Phytother. Res. 29 (6), 796–804. https://doi.org/10.1002/ptr.5325.

Taesotikul, T., Navinpipatana, V., Tassaneeyakul, W., 2010. Selective inhibition of human cytochrome P450 1A2 by *Moringa oleifera*. Thai. J. Pharmacol. 32, 256–258.

Valentova, K., Vrba, J., Bancirova, M., Ulrichova, J., Kren, V., 2014. Isoquercitrin: pharmacology, toxicology, and metabolism. Food Chem. Toxicol. 68, 267–282. https://doi.org/10.1016/j.fct.2014.03.018.

Zulfiqar, F., Khan, S.I., Ross, S.A., Ali, Z., Khan, I.A., 2017. Prenylated flavonol glycosides from *Epimedium grandiflorum*: cytotoxicity and evaluation against inflammation and metabolic disorder. Phytochem. Lett. 20, 160–167. https://doi.org/10.1016/j.phytol.2017.04.027.